Large Volume Self-powered Disposable Microfluidics by the Integration of Modular Polymer Micropumps with Plastic Microfluidic Cartridges

J. Etxebarria-Elezgarai[1†±], Y. Alvarez-Braña[1,2†], R. Garoz-Sanchez[1,2], F. Benito-Lopez[1,2], L. Basabe-Desmonts[1-3*]

[1]BIOMICs microfluidics Research Group, Microfluidics Cluster UPV/EHU, Lascaray Research Center, University of the Basque Country UPV/EHU, Avenida Miguel de Unamuno, 3, 01006 Vitoria-Gasteiz, Spain

[2]Analytical Microsystems & Materials for Lab-on-a-Chip (AMMa LOAC) Group, Microfluidics Cluster UPV/EHU, University of the Basque Country UPV/EHU, Paseo de la Universidad, 7, 01006 Vitoria-Gasteiz, Spain

[3]Basque Foundation of Science, IKERBASQUE, María Díaz Haroko Kalea, 3, 48013 Bilbao, Spain

± Current address at: CIC NanoGUNE, Tolosa Hiribidea, 76, 20018 Donostia, Gipuzkoa, Spain

† Both authors contributed iqually to this work.

ABSTRACT

Microfluidic microsystems are often designed to analyse samples of small volume of fluid, however, some applications require the analysis of larger volumes. The ideal miniaturized microfluidic analytical device should be autonomous and capable of integrating all the required functions within a single fluidic network. While a number of self-powered microfluidic networks designs are available, the autonomous manipulation of large sample volumes in microsystems is still a challenge. We have developed a universal self-powered microfluidic architecture by combining polymeric micropumps and plastic microfluidic cartridges, which may be adapted to a large range of volume of fluid. Our polymeric micropumps were able to trigger flow rates from 0.25 to 20 $\mu L \cdot min^{-1}$ during more than 40 minutes, moving over 800 microliters of fluid. A number of fluidic operations were demonstrated, including: mixing, aliquoting, waste storage and auto-draining of the microfluidic channels. Finally, a self-powered cartridge for the separation of plasma from whole blood was successfully validated, demonstrating that this constitutes a universal scheme to process a wide range of fluid volumes, an unprecedented fact in self-powered microfluidics.

KEYWORDS: Self-powered microfluidics, multilayer microfluidics, micro-pumps, fluidic operations, modular microfluidics, micro-trench, whole blood.

1. **INTRODUCTION**

Lab on a chip technology provides the means to perform all the steps of an analytical process such as sample collection, sample preparation and analysis, in a single device. In order to enhance the automation of the process, the ideal miniaturised analytical device should be autonomous and able to integrate all the required analytical functions within a single microfluidic network [1]. Flow control is often a critical aspect in microfluidic devices, since it controls residence times and shear forces, among others. Flow is often controlled using conventional peristaltic or syringe pumps and pressurized flow controllers, which are generally bulky components that require external power sources. In contrast, the integration of micropumps within the microfluidic network renders self-powered autonomous devices in which flow does not depend on external components [2,3]. Finger actuated pumps [4,5], capillary driven flows [6,7], paper driven flows [8,9] (including paper lateral flows), threads-based devices [10,11], and in particular, stimuli responsive [12,13] or vacuumed materials [14,17] are being integrated within microfluidic devices for fluid manipulation and flow control at the microscale. In some of these devices, like finger-actuated devices, it is difficult to precisely control the flow [7], while others allow to have a predetermined flow. However, the design of the latest devices must be completely modified in order to change the flow, increasing the manufacturing time. This is the case of capillary on vacuum driven devices like SIMBAS [14]. In 2012, Zhao et al. reported modular PDMS Plug and Play (PnP) micropumps [18]. These modular micropumps could be designed and connected to a microfluidic device to promote controlled flows within the microchannels due to the negative pressure produced by degassed-PDMS [19]. The pressure produced by those micropumps could be tuned by controlling certain parameters such as surface area and volume of PDMS, which allowed to control the flow on microfluidic devices by a polymeric modular micropump. However, their devices were focussed on moving samples of small volume, and their micropumps could only produce flow rates in the range of $nL \cdot min^{-1}$ in a Teflon tube with an inner diameter of 0.5 mm.

While it is common that microsystems are designed to analyse small sample volumes, several biomedical and environmental applications that pursue the detection of analytes present at very low concentrations require to process larger volumes of fluid. For example, circulating tumour cells (CTC´s) are present in the circulation torrent at a concentration of 1-10 cell $\cdot mL^{-1}$ in early disease stages and, therefore, at least 1 mL of blood must be analysed in order to detect a single CTC [20]. This is also the case when trying to detect nucleic acids, proteins, bacteria or viruses in blood [21]. For the analysis of environmental samples, the target analytes such as waterborne pathogens from drinking water or heavy metals and toxic gases from industrial effluents are typically in the range of parts per million (ppm) or parts per billion (ppb), therefore, their detection often requires a preconcentration step [22]. Current self-powered microsystems are normally only suitable to process a maximum of a few microliters, preventing their use for this type of applications.

Additionally, the fabrication of plastic microfluidic cartridges by multilayer lamination of grafted plastic sheets followed by compression is a highly versatile, easy and rapid prototyping methodology compared to other methods currently used [23-28]. In order to make it accessible to any laboratory, we recently investigated the lamination of grafted plastic layers using interpenetrated pressure sensitive adhesive (PSA) layers for bonding. It has been shown that by just applying low pressures for bonding and sealing the layers comprising the device, this technique enables the fabrication of both 2D and 3D microfluidic networks, which stand up to 1000 mbar, within minutes [29, 30].

In order to overcome the limitations of the autonomous motion of large volumes of fluid within microfluidic devices at a controlled flow rate, we explored the fabrication of large area (LA) PDMS micropumps and their combination with the multilayer lamination technique. This strategy makes it possible to fabricate disposable cartridges that are able to process sample volumes above 500 μL, as well as controlling the autonomous flow provided by the PDMS micropumps.

Herein, we present the integration and performance of modular LA-PDMS micropumps with microfluidic cartridges produced by multilayer lamination of grafted plastic substrates, Figure 1. The versatility of this strategy for fast prototyping is demonstrated by autonomous microfluidic devices, which are designed for a number of commonly used microfluidic operations using 2D and 3D microfluidic networks such as mixing, aliquoting and sequential flow. Finally, we also evaluated the performance of these modular devices, as a proof of principle, for the autonomous extraction of plasma from whole blood.

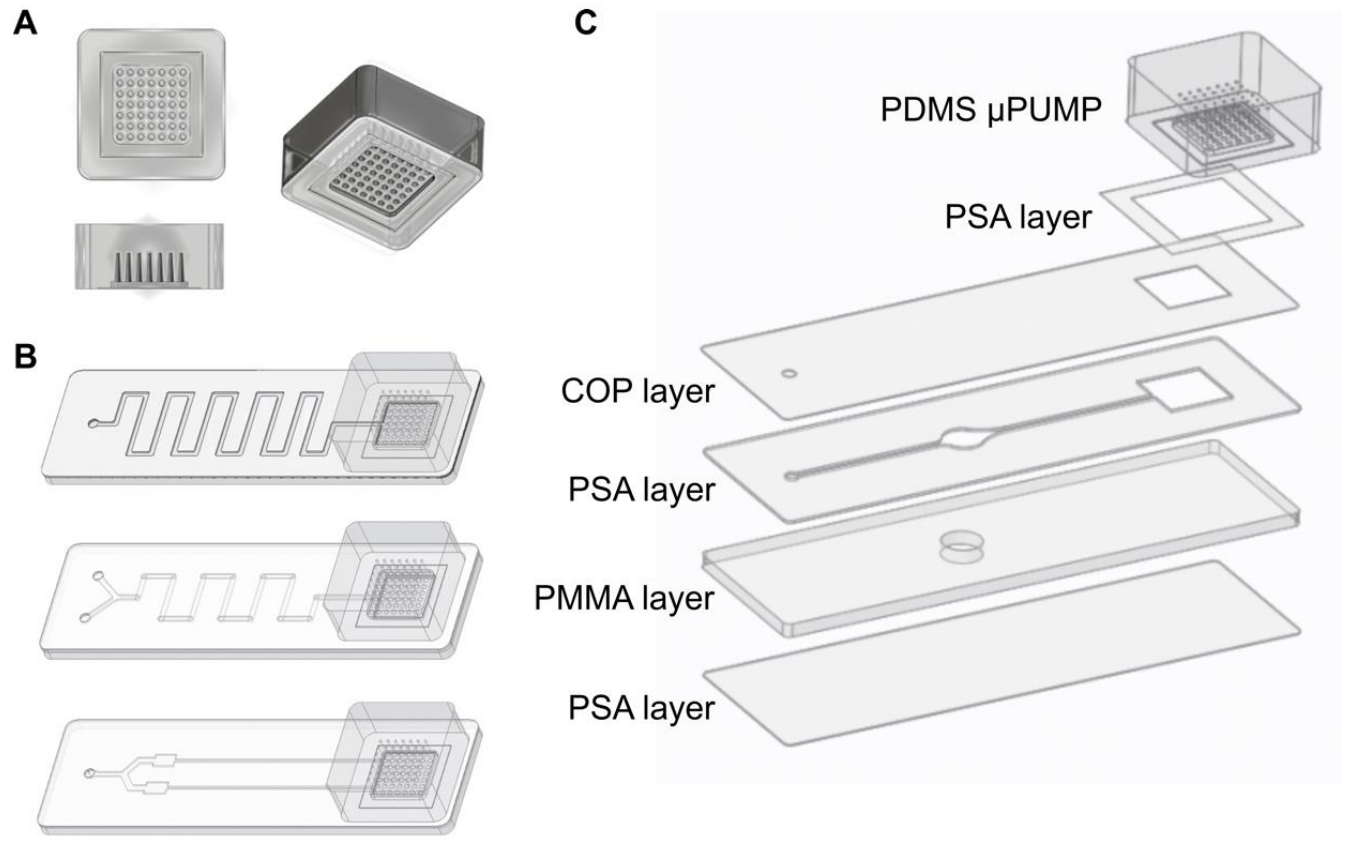

Figure 1. A) Modular PDMS micropumps enable different fluidic operations in a modular approach. B) Several plastic multilayer microfluidic cartridges with integrated PDMS micropumps. C) Schematic representation of the lamination method employed to manufacture the multilayer microfluidic devices.

2. MATERIALS AND METHODS

2.1. PDMS micropumps fabrication

The PDMS micropumps were fabricated by casting, using the SYLGARD 184 silicone elastomer kit (Farnell, Spain). The curing agent and the polymer-base were mixed in 1:10 or 1:20 proportions and degassed in a vacuum desiccator (PolyLab, Spain) for 30 min to remove air bubbles generated during mixing. Once degassed, the PDMS mixture was poured onto a negative mold (fabricated by microLIQUID, Spain) containing 49 pillars (R_1 = 0.50 mm, R_2 = 0.25 mm, H = 4.00 mm), and fabricated by stereolithography 3D printing. Next, the mold was placed at 70 °C in a STZ 5.4 mini oven (FALC, Italy) for 2 h in order to fully cross-link the PDMS and the resulting part was peeled off from the mold. The finalized PDMS micropumps, which are composed of one or several micropump units, are shown in Figure 2A, and the mold used for PDMS casting is depicted in Figure S1A. The effective surface area of each unit, including the surface of the chamber sidewall, the ceiling and the 49 cavities contained in the unit, was calculated to be 683 mm^2. 146 µm thick ARcare® 90880 transparent Pressure Sensitive Adhesive (PSA) (Adhesive Research, Ireland) was employed to assemble the different units, as well as to seal the micropumps to the microfluidic devices. To assemble and connect multiple units, four through-holes were manually punched in the intermediate units, using a 2.0 mm diameter Harris Uni-core puncher (Sigma Aldrich, Spain), see Figure 2A.

2.2. Micropumps actuation and characterisation

Manufactured PDMS micropumps were degassed in a RVR003H-01Vacuum Chamber (Dekker Vacuum Technologies, USA) for 2 h at 0.7 mbar, and vacuum packed in a SV-204 vacuum sealer (Sammic, Spain) in order to store in airless environment. This vacuum-packed process is independent of the plastic cartridges and allows storage and transport of the pumps for long periods of time, ready to use.

The flow profiles induced by the micropumps over time were measured with a flow characterization setup (see Figure S1B) by mounting the micropumps onto a 3D printed acrylic microfluidic device. Next, the characterization device was connected to a flow sensor (Flow-Rate Platform, Fluigent Smart Microfluidics) using a P-675 1/4-28 female to male luer (Upchurch Scientific (IDEX Health & Science), USA) and a 200 mm long transparent Tubing (1/16 OD, 0.020/0.5mm ID, FEP) (Vici Valco, Canada). The Flow sensor and the fluidic circuit were connected using 90 mm of 1/32'' OD x0.010'' ID PEEK blue tubing and 1/16" OD to 1/32" OD ZDV PEEK adapters (Upchurch Scientific (IDEX Health & Science), USA). A rectangular shaped PSA was used to assure a leak-free sealing between the micropump and the acrylic device.

2.3. Fabrication of 3D printed acrylic microfluidic devices

The devices were printed as a single piece in the Form 1+ 3D printer (Formlabs, U.S.A.), using a 100 µm printing resolution and an optically clear acrylic material (Clear resin FLGP CL02, Formlabs, U.S.A.). The parts were designed using Creo PTC and PreForm software. After printing, the devices were rinsed in isopropanol for 4 min and post-cured under UV at 365 nm for 30 min. The supports were removed using a snip and wet sandpolish was carried out to enhance transparency.

2.4. Fabrication of multilayer-plastic microfluidic cartridges

Plastic cartridges were fabricated by multiple-layer lamination. Microfluidic channels were cut by Graphtec cutting Plotter CE6000-40 (CPS Cutter Printer Systems, Spain) on sheets of Cyclic Olefin Polymer layers (COP) (188 µm mcs-COP-02, Microfluidic ChipShop) and on sheets of Pressure Sensitive Adhesive layers (127 µm thick ARcare® 8939 white PSA, 50 µm thick ARcare® 92712 transparent PSA and 146 µm thick ARcare® 90880 transparent PSA). A 1.1 mm thick PMMA substrate (ME303010, clear, Goodfellow) was used as the bottom base of the device. The PMMA layer was grafted by a CO_2 Laser System (VERSA Laser, VLS2.30 Desktop Universal Laser System equipped with one 10.6µ CO_2 laser

source ranging in power from 10 to 30 watts). All the cartridges included a 10 x 10 mm waste reservoir at the end of the channels in the PMMA layer. The assembly and lamination of the COP, PSA and PMMA layers, one on top of the other, generated the 2D and the 3D microfluidic networks. A COP layer and a transparent PSA layer were used to seal the device and to cover the structures from the top and bottom, respectively (Figure 1B and 1C). To facilitate sample loading, a liquid reservoir was assembled on the inlet port of the cartridges (Female Luer Lok compatible connector with wide base, PMMA, microfluidic ChipShop). The top COP layer also included a small venting hole of 2 mm diameter close to the outlet port. The purpose of the venting port is to control the onset of flow inside the microchannels when the micropump is mounted in the cartridge. When the port is opened, the micropump gets air from outside of the device, while, when it is closed, the micropump absorbs the air from the microchannel and triggers the flow inside the channel.

2.5. Fabrication of multilayer-plastic cartridges for plasma separation

As in the previous case, plastic cartridges were fabricated by multiple-layer lamination. Microfluidic channels were cut by Graphtec cutting Plotter CE6000-40 on sheets of Pressure Sensitive Adhesive layers (PSA) (127 µm thick ARcare® 8939). The bottom base of the device, a 4 mm thick PMMA substrate (PLEXIGLAS®, Evonik Industries AG), included the waste reservoir at the end of the channels and a filtration trench in the middle of the channel, grafted by a CO_2 Laser System. The top layer was cut on sheets of Cyclic Olefin Polymer layers (COP) (188 µm mcs-COP-02, Microfluidic ChipShop) and a layer of transparent PSA was used to seal the bottom and top of the trench and other structures. A round shape of PMMA piece was used as a reservoir to load the blood sample and a layer of PSA (146 µm thick ARcare® 90880 transparent PSA) was used to assemble the PDMS µPump.

2 mL of blood were collected in a 3.2% sodium citrate vacuum tube from BD Vacutainer® System. Blood was obtained from volunteer healthy donors and used within a period of 2 days from extraction.

2.6. Evaluation of self-powered cartridge performance

Aqueous food colour solutions (McCormick, Sabadell, Spain) were loaded into the self-powered multilayer devices. Upon closing of the venting port by a PSA sheet, flow is triggered inside the microchannels. Flow was evaluated by acquiring images and videos with a digital camera (DCS-RX100, SONY).

3. RESULTS AND DISCUSSION

3.1. Large surface area PDMS micropumps

Degassed PDMS micropumps were able to absorb air from a closed system into the PDMS. This absorption process produced a negative pressure that triggered the movement of fluid inside a microchannel. Previous reports by Zhao *et al.* [18] showed that the pressure generated by their PDMS was proportional to the effective surface area of the micropump; however, those micropumps produced flow rates only in the range of the $nL \cdot min^{-1}$ in a Teflon tube with an inner diameter of 0.5 mm.

In order to increase the flow rate that a micropump could produce, we undertook the design and fabrication of novel PDMS micropumps with large surface areas, which we named LA-PDMS micropumps. In our experiments, a micropump was comprised of one or multiple units, where each unit has an effective total surface area of approximately 683 mm^2 per unit (see table SI-1). By combining 2, 3 or 4 units, it was possible to increase the surface area of the final micropumps from 683 up to 1818, 2952 and 4087 mm^2, respectively. Measuring the flow rates generated by each micropump, we observed a rapid increase to their maximum value in the first few minutes of operation. The time needed to achieve the maximum flow rate ranged from 30 s to 4 min, increasing with the number of units. After that, the flow rate decayed with

a double exponential waveform for several minutes before getting into a slow decay regime. In the slow decay domain, after 30 min of operation, flow rates of 1, 3, 6 and 9 $\mu L \cdot min^{-1}$ were measured for micropumps with 1, 2, 3 and 4 units, respectively (Figure 2B and Figure S2). The intra-variability of the performance of the micropumps (same micropump tested several times (n=3)) was less than 9%, and the inter-variability of identical micropumps fabricated at different times, was less than 12 %. Additionally, it was observed that the lower the number of units in the micropump, the faster the transition to the slow decay domain was, resulting in less variable flow rates. For all micropumps, after ten minutes of operation the flow was fairly stable with a 2% decay per minute (Figure S5)

Another series of micropumps with different degree of cross linking, 1:20 (curing agent : polymer), were fabricated in order to prove that decreasing amounts of the curing agent lead to less cross-linking, and thus more free internal air volume in the PDMS. With this set of pumps, the same flow rate behaviour was observed in which a rapid increase in flow rate was followed by a decay with a double exponential waveform for several minutes before getting into a slow decay regime, Figure S3. However, in this case, the maximum flow rate and the flow rate in the slow decay domain were higher than in the previous experiments, as can be seen in Figure S4. This agrees with Zhao´s work, where they showed that a higher cross-linking rate of the PDMS is related to a lower permeability of the material.

Figure 2C shows the linear relation of the average flow rate generated by the micropumps with respect to the number of units. The times of activity of the micropumps ranged from 35 to 90 min, which were considerably lower than the activity times of Zhao´s micropumps. This may be explained by the difference in S:V ratio. In other words, our micropumps had a volume of approximately 4000 mm^3 per unit with areas of 683, 1818, 2952 and 4087 mm^2 for 1, 2, 3 and 4 units, respectively. From these data, the calculated S:V values were 0.1687 mm^{-1} for 1 unit, 0.2275 mm^{-1} for 2 units, 0.2475 mm^{-1} for 3 units and 0.2576 mm^{-1} for 4 units (see Table SI-1). These values are approximately 60 times bigger than in Zhao´s pumps,

therefore, a smaller S:V ratio resulted in a larger time of activity. These results indicated that it could be possible to tune the duration of the micropump activity by varying the ratio between effective surface area and the volume of PDMS (S:V).

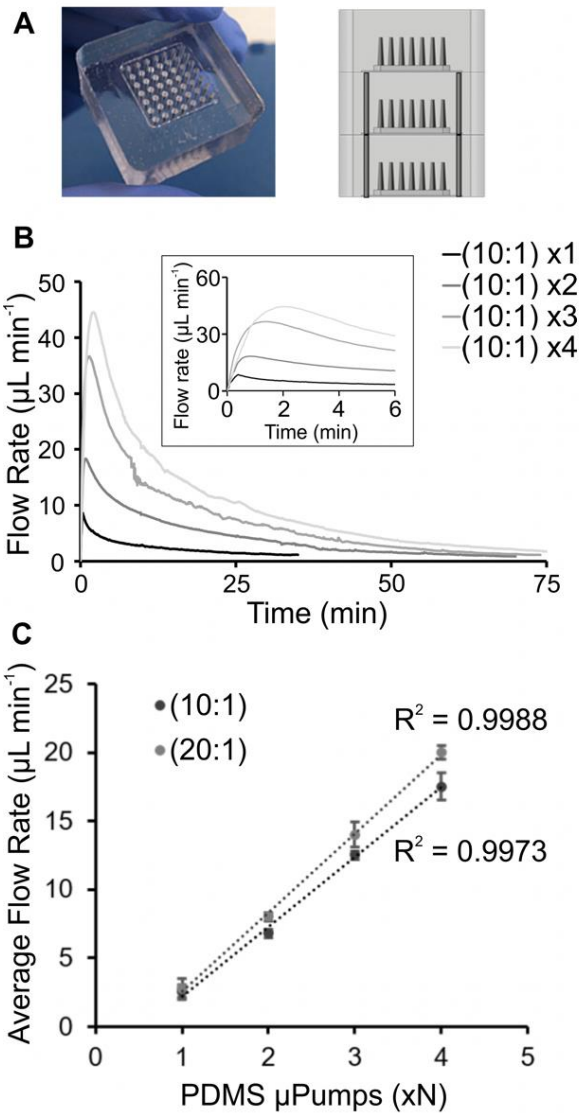

Figure 2. A) Picture of one PDMS micropump unit and scheme of the assembly of different units, where the through-holes made in the stacked units allow interconnection among units. B) Measurements of flow rate generated over time by micropumps with 1, 2, 3 and 4 units, fabricated from curing agent : elastomer

mixtures of 1:10, during 90 min. The inset shows the first 6 minutes of operation of all different micropumps. C) Average flow rate generated by the micropumps fabricated from curing agent : elastomer mixtures of 1:10 and 1:20, with respect to the number of units.

Finally, we evaluated the volume of liquid that the micropumps could displace. Our 1:20 micropumps, comprised of 1, 2, 3 and 4 units, were able to displace approximately 109 μL, 351 μL, 619 μL and 878 μL respectively. The amount of liquid that the micropump could displace is determined by the flow rate generated by the micropump and its activity time. These results demonstrated that these micropumps could be used to pump a wide range of volumes of fluids up to the millilitre range, by just varying the effective surface area to volume ratio (S:V), an unprecedented and highly relevant fact in self-powered microfluidics.

3.2. Autonomous multilayer microfluidic devices

In order to evaluate if LA-PDMS micropumps could produce enough pressure difference to promote controlled microfluidic flow within multilayer microfluidic devices, several pumps were assembled to multilayer plastic cartridges containing both 2D and 3D microfluidic networks. First, two different pre-vacuumed micropumps (a single unit pump and a double unit pump) were attached to two identical cartridges comprised of a single 2D microchannel with dimensions: 0.254 mm (height) x 1 mm (width) x 150 mm (length), see Figure 3A. Upon loading of the sample and closing of the vent, both pumps onset autonomous flow inside each microchannel. The double unit pump induced a faster flow rate within the microchannel than in the case of the single unit pump, see Figure S6, and Video S1. Sequential addition of coloured samples at the inlet in a one unit pump device resulted in segmented fluid plugs that flowed through the same microchannel independently from each other, see Figure 3B and Video S2.

The possibility of making aliquots from a sample using this type of devices was also investigated. A cartridge with a single inlet channel divided into two channels was fabricated using the lamination technique. Each channel was comprised of three regions, a lower flow resistance region, an aliquot reservoir, and a higher flow resistance area at the exit of the aliquot reservoirs. Upon sample loading, we successfully achieved autonomous flow within the cartridge and the splitting of the sample in two identical aliquots, see Figure 3D.

Finally, we designed a mixing cartridge. A 3D microfluidic cartridge was fabricated to evaluate the self-powered mixing of liquids into a single microchannel (see Figure S7B for device design). Two different colour solutions were loaded into two different inlets, and upon closure of the vent, the liquid flowed through the cartridge microchannel producing turbulence and mixing of both liquids due to the 3D structure of the serpentine, see Figure 3C and Video S3. The 3D structure of the microchannels enabled an efficient mixing in contrast to a 2D serpentine of the same length, where the laminar flow prevented the mixing of the fluids (Figure S7A)

In every case, the liquid flowed through the microchannels until reaching the reservoir under the micropump. The microchannels emptied without any user intervention and the liquid did not get in touch with the micropump in any case. In conclusion, this configuration allowed the micropump to continue driving the flow of liquid independently of the volume passing through the microchannel.

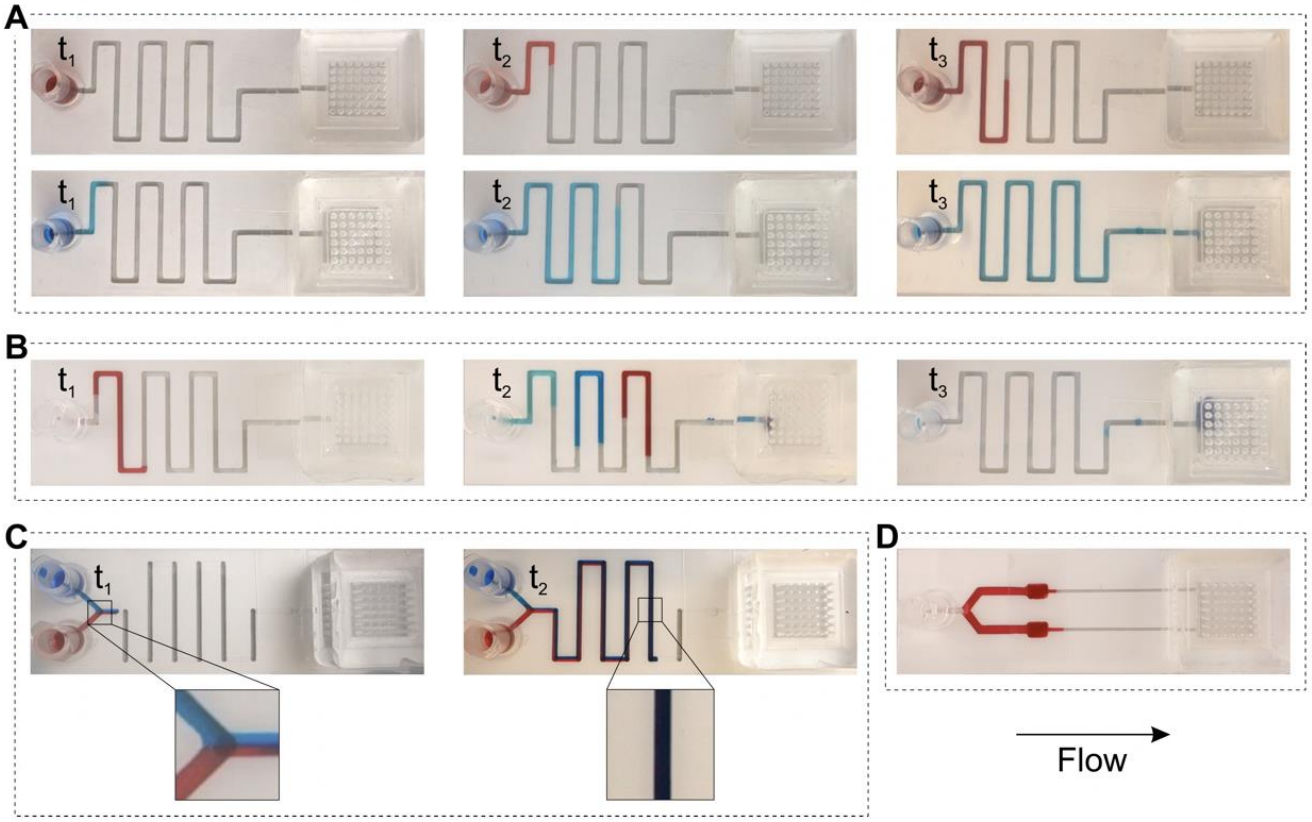

Figure 3. Self-powered cartridges during operation. A) Single channels cartridges assembled to a micropump containing 1 unit (top) or 2 units (bottom) after 5 s (t_1), 25 s (t_2) and 50 s (t_3) of operation, demonstrating that the flow rate obtained with the 2 units is greater than with 1 unit (see Figure S6 and Video S1). B) Single channel cartridge assembled to a micropump containing 1 unit after 12 s of operation, when only an aliquot of red fluid was added (t_1), and after 2 min of operation, when three fluid plugs have been sequentially loaded (t_2) (see Video S2). C) Sequence of images of a cartridge during the mixing of two-coloured fluids after 32 s (t_1) and 90 s (t_2) of operation (see Figure S7 for design and Video S3). D) Aliquoting cartridge producing two aliquots from a single sample after 100 s of operation.

3.3. Whole blood plasma preparation in an autonomous microfluidic system

In clinical laboratories, where the accurate analysis of plasma components is fundamental in the diagnosis and monitoring of diseases, the precise separation of plasma from blood cells is a crucial process. This

process is usually conducted by centrifugation. As previously stated, the development of new devices for sensitive diagnosis of certain diseases should enable the analysis of blood samples of larger volumes than a few microliters, in order to allow the detection of low concentration analytes, what would not be possible with just a drop of blood [20]. As a proof of concept, we evaluated the use of our self-powered plastic cartridges assembled to PDMS micropumps to perform the separation of plasma and red blood cells from whole blood. Inspired by a previous design of a microfluidic device made of PDMS to process small volumes of blood [14], a multilayer cartridge comprised of a single microchannel of 35 mm long and a round micro-trench of 6 mm diameter and 4 mm depth (total trench volume of 115 mm^3) was fabricated, see Figure 4A. The cartridge was assembled to a 2 units micropump that produced an average flow rate of 13 $\mu L \cdot min^{-1}$. 250 µL of whole blood were loaded into the cartridge and blood flowed through the channel and the trench. After 30 min, cells settled into the trench and only plasma overflowed and continued through the microchannel until the final reservoir. A total amount of 60 µL of plasma were recovered at the reservoir. Therefore a 44% of the total plasma in the sample was extracted.

The purity of the plasma was characterized by comparing the number of red and white blood cells in the plasma and in the original blood sample. In the blood sample, the concentration of RBCs was 4.84×10^6 cells $\cdot \mu L^{-1}$ and the concentration of WBCs was 5.35×10^3 cells $\cdot \mu L^{-1}$, while the concentrations of RBCs and WBCs in the plasma were 3.00×10^4 cells $\cdot \mu L^{-1}$ and 3.12×10^3 cells $\cdot \mu L^{-1}$, respectively. Thus, 99 % of the RBCs and 42 % of the WBCs were retained in the trench and eliminated from the extracted plasma.

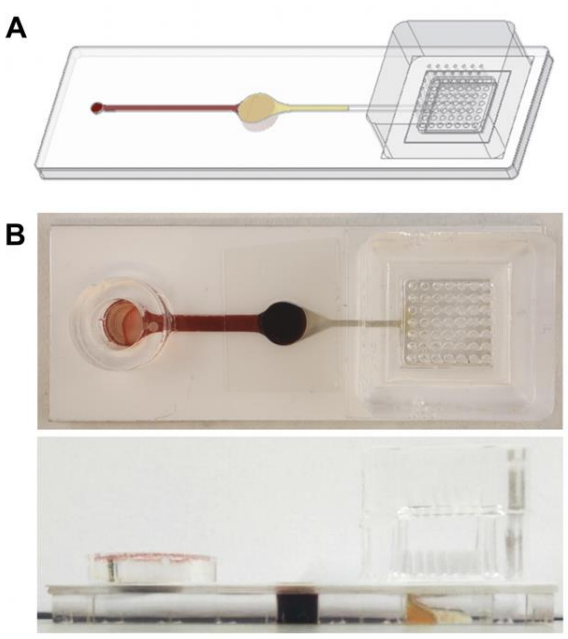

Figure 4. A) Scheme of the plastic multilayer cartridge with a PDMS micropump attached. B) Top and side views of the device during the separation of 250 µL of blood.

4. CONCLUSIONS

Herein, we have introduced a highly versatile architecture for self-powered microfluidics adaptable to a large range of fluid volumes. For the first time, Large Area PDMS micropumps are reported. In agreement with previous reports, these LA-PDMS micropumps generated higher flow rates when the effective surface area to volume ratio (S:V) values and/or the permeability degree of the PDMS were increased. These micropumps can be customized by increasing the number of constituting units, enabling the user to obtain the desired flow rate, which can last for hours, in order to match the specifications of each application. As it can be seen in this work, LA-PDMS micropumps of 4 modules showed, for the first time, 90 min of autonomous flow of more than 800 µL of sample through a single microchannel.

In addition, the combination of modular polymeric micropumps with multilayer plastic microfluidic cartridges is as a highly versatile strategy for the development of self-powered microfluidic devices, since it allows a fast change of the cartridge's design and the re-use of the micropumps at the prototyping stage, when the production of few units is pursued. As a proof of concept, this methodology was validated with the fabrication of a microfluidic cartridge combined with LA-PDMS micropumps to be used for the integration of several steps of blood analysis in a single device such as plasma separation, plasma transport and plasma storage. This experiment not only demonstrates the use of self-powered devices for possible applications in diagnosis of large biological samples, but it also shows the use of a liquid more viscous than water as a sample. The performance of the micropump is independent of the properties of the liquids flowing inside the microchannels. The ease of fabrication of these devices allows to include different structures within the microfluidic channel, such as waste/collection reservoirs, providing the means not only for self-storage of waste or sample collection, but also to avoid dead volumes. Overall, the combination of polymeric micropumps with multilayer plastic microfluidic cartridges overtakes in a simple manner many limitations present in other self-powered devices, which are restricted to very small sample volumes and where it is difficult to integrate fluidic operations, demonstrating also its potential for applications where greater flow control is required.

5. ACKNOWLEDGEMENTS

Authors would like to acknowledge the University of the Basque Country (ESPPOC 16/65); the Gobierno de España, Ministerio de Economia y Competitividad, with Grant No. BIO2016-80417-P. We acknowledge funding support from Gobierno Vasco, Dpto. Industria, Innovación, Comercio y Turismo under ELKARTEK 2017 with Grant No. KK-2017/0000088 and Gobierno Vasco Dpto. Educación for the consolidation of the research groups (IT1271-19). LBD and FBL personally

acknowledge funds from the DNASURF (H2020-MSCA-RISE-778001) project. Authors thank for technical and human support provided by PhD Maite Alvarez from DNA Bank Service (SGIker) of the University of the Basque Country (UPV/EHU) and European funding (ERDF and ESF).

6. SUPPORTING INFORMATION

- Word document containing the figures:
    - Figure S1: Master mold for the PDMS micropumps and setup for flow rates measurements over time.
    - Table S1: Table with the specifications of the large surface PDMS micropumps described in this manuscript.
    - Figure S2: Set of characterization measurements of flow rate generated over time by micropumps with 1, 2, 3 and 4 units, fabricated from curing agent : elastomer mixtures of 1:10.
    - Figure S3: Set of characterization measurements of flow rate generated over time by micropumps with 1, 2, 3 and 4 units, fabricated from curing agent : elastomer mixtures of 1:20.
    - Figure S4: Measurements of flow rates and maximum flow rate generated by the micropumps with respect to the number of units and the grade of cross-linking.
    - Figure S5: Measurements of flow rates generated from 10 to 12 min with 1, 2, 3 and 4 units, fabricated from curing agent : elastomer mixtures of 1:10.
    - Figure S6: Time variation of liquid delivery volume in the speed assay for a single unit pump and a double unit pump.

- Figure S7: Scheme of the multilayer composition of the 3D microfluidic cartridge to promote mixing of fluids.

- Supporting videos of:
  - Video S1: Speed Assay Speed Assay - Single channels cartridges assembled to 1 micropump unit and to 2 micropump units to create a different flow inside the devices, with the same microchannel dimensions.
  - Video S2: Sequential Addition Assay - Single channel cartridge for the sequential loading of three fluids.
  - Video S3: Mixing Assay - 3D microfluidic cartridge to promote mixing of fluids.

7. CONFLICTS OF INTEREST

The authors declare no competing financial interest.

8. REFERENCES

[1] St John, A.; Price, C. P. Existing and Emerging Technologies for Point-of-Care Testing, *Clin. Biochem. Rev.* **2014,** *35*, 155-167.

[2] Sengupta, S.; Patra, D.; Ortiz-Rivera, I.; Agrawal, A.; Shklyaev, S.; Dey, K. K.; Córdova-Figueroa, U.; Mallouk, T. E.; Sen, A. Self-powered enzyme micropumps, *Nat. Chem.* **2014,** *6*, 415-422.

[3] Zhou, C.; Zhang, H.; Li, Z.; Wang, W. Chemistry pumps: a review of chemically powered micropumps, *Lab Chip* **2016,** *16*, 1797–1811.

[4] Iwai, K.; Shih, K. C.; Lin, X.; Brubaker, T. A.; Sochol, R. D.; Lin, L. Finger-powered microfluidic systems using multilayer soft lithography and injection molding processes, *Lab Chip* **2014,** *14*, 3790-3799.

[5] Park, J.; Park, J-K. Integrated microfluidic pumps and valves operated by finger actuation, *Lab Chip* **2019,** *19,* 2973-2977.

[6] Gökçe, O.; Castonguay, S.; Temiz, Y.; Gervais, T.; Delamarche, E. Self-coalescing Flows in Microfluidics for Pulse-Shaped Delivery of Reagents, *Nature* **2019,** *574,* 228-232.

[7] Arange, Y.; Temiz, Y.; Gökce, O.; Delamarche, E. Electro-actuated valves and self-vented channels enable programmable flow control and monitoring in capillary-driven microfluidics, *Sci. Adv*. **2019,** *6,* eaay8305.

[8] Akyazi, T.; Basabe-Desmonts, L.; Benito-Lopez, F. Review on microfluidic paper-based analytical devices towards commercialisation, *Anal. Chim. Acta* **2018,** *1001,* 1-17.

[9] Jang, I.; Carrao, D.; Menger, R.; Moraes de Oliveira, A. R.; Henry, C. S. Pump-free microfluidic rapid mixer combined with a paper-based channel, *ACS Sens.* **2020,** *5,* 2230–2238.

[10] Curto, V. F.; Coyle, S.; Byrne, R.; Angelov, N.; Diamond, D.; Benito-Lopez, F. Concept and development of an autonomous wearable micro-fluidic platform for real time pH sweat analysis, *Sens. Actuators, B* **2012,** *175,* 263-270.

[11] Delon, L. C.; Nilghaz, A.; Cheah, E.; Prestidge, C.; Thierry, B. Unlocking the potential of organ-on-chip models through pumpless and tubeless microfluidics, *Adv. Healthcare Mater.* **2020,** *9,* 1901784.

[12] Delaney, C.; McCluskey, P.; Coleman, S.; Whyte, J.; Kent, N.; Diamond, D. Precision Control of Flow Rate in Microfluidic Channels Using Photoresponsive Soft Polymer Actuators, *Lab Chip* **2017,** *17*, 2013-2021.

[13] Akyazi, T.; Tudor, A.; Diamond, D.; Basabe-Desmonts, L.; Florea, L.; Benito-Lopez, F. Driving flows in microfluidic paper-based analytical devices with a cholinium based poly(ionic liquid) hydrogel, *Sens. Actuators, B* **2018,** *261,* 372-378.

[14] Dimov, I. K.; Basabe-Desmonts, L.; Garcia-Cordero, J. L.; Ross, B. M.; Ricco, A. J.; Lee, L. P. Stand-alone Self-powered Integrated Microfluidic Blood Analysis System (SIMBAS), *Lab Chip*. **2011,** *11,* 845-850.

[15] Liu, Y.; Li, G. A power-free parallel loading microfluidic reactor array for biochemical screening, *Sci. Rep.* **2018,** *8,* 13664.

[16] Narayanamurthy, V.; Jeroish, Z. E.; Bhuvaneshwari, K. S.; Bayat, P.; Premkumar, R.; Samsurie, F.; Yusoff, M. M. Advances in passively driven microfluidics and lab-on-chip devices: a comprehensive literature review and patent analysis, *RSC Adv.* **2020,** *10,* 11652-11680.

[17] Yeh, E.; Fu, C.; Hu, L.; Thakur, R.; Feng, J.; Lee, L. P. Self-powered integrated microfluidic point-of-care low-cost enabling (SIMPLE) chip, *Sci. Adv.* **2017,** *3,* e1501645.

[18] Li, G.; Luo, Y.; Chen, Q.; Liao, L.; Zhao, J. A "place n play" modular pump for portable microfluidic applications, *Biomicrofluidics* **2012,** *6,* 014118(01)-014118(16).

[19] Xu, L.; Lee, H.; Jetta, D.; Oh, K. W. Vacuum-driven power-free microfluidics utilizing the gas solubility or permeability of polydimethylsiloxane (PDMS), *Lab Chip* **2015,** *15,* 3962-3979.

[20] Nagrath, S.; Sequist, L. V.; Maheswaran, S.; Bell, D. W.; Irimia, D.; Ulkus, L.; Smith, M. R.; Kwak, E. L.; Digumarthy, S.; Muzikansky, A.; Ryan, P.; Balis, U. J.; Tompkins, R. G.; Haber, D. A.; Toner, M. Isolation of Rare Circulating Tumour Cells in Cancer Patients by Microchip Technology, *Nature* **2007,** *450,* 1235-1239.

[21] Amasia, M.; Madou, M. Large-volume Centrifugal Microfluidic Device for Blood Plasma Separation, *Bioanalysis* **2010,** *2,* 1701-1710.

[22] Yew, M.; Ren, Y.; Koh, K. S.; Sun, C.; Snape, C. A Review of State- of- the- Art Microfluidic Technologies for Environmental Applications: Detection and Remediation, *Global Challenges* **2019,** *3,* 1800060.

[23] Carbonell, C.; Valles, D.; Wong, A. M.; Carlini, A. S.; Touve, M. A.; Korpanty, J.; Gianneschi, N. C.; Braunschweig, A. B. Polymer brush hypersurface photolithography, *Nat. Commun.* **2020,** *11,* 1244.

[24] Etxebarria, J.; Berganzo, J.; Elizalde, J.; Fernández, L. J.; Ezkerra, A. Highly integrated COP monolithic membrane microvalves by robust hot embossing, *Sens. Actuators, B* **2014,** *190,* 451-458.

[25] Johnson, T. J.; Waddell, E. A.; Kramer, G. W.; Locascio, L. E. Chemical mapping of hot-embossed and UV-laser-ablated microchannels in poly(methyl methacrylate) using carboxylate specific fluorescent probes, *Appl. Surf. Sci.* **2001,** *181,* 149-159.

[26] Hu, X.; Yang, F.; Guo, M.; Pei, J.; Zhao, H.; Wang, Y. Fabrication of polyimide microfluidic devices by laser ablation based additive manufacturing, *Microsyst. Technol.* **2020,** *26,* 1573-1583.

[27] Bhattacharjee, N.; Urrios, A.; Kang, S.; Folch, A. The upcoming 3D-printing revolution in microfluidics, *Lab Chip* **2016,** *16,* 1720-1742.

[28] Bhattacharjee, N.; Parra- Cabrera, C.; Kim, Y. T.; Kuo, A. P.; Folch, A. Desktop-Stereolithography 3D-Printing of a Poly(dimethylsiloxane)-Based Material with Sylgard-184 Properties, *Adv. Mater.* **2018,** *30,* e1800001.

[29] Saez, J.; Basabe-Desmonts, L.; Benito-Lopez, F. Low-cost Origami Fabrication of 3D Self-aligned Hybrid Microfluidic Structures, *Microfluid. Nanofluid.* **2016,** *20,* 1-7.

[30] Yuen, P. K.; Goral, V. N. Low-cost rapid prototyping of flexible microfluidic devices using a desktop digital craft cutter, *Lab Chip* **2010,** *10,* 384-387.

TABLE OF CONTENTS

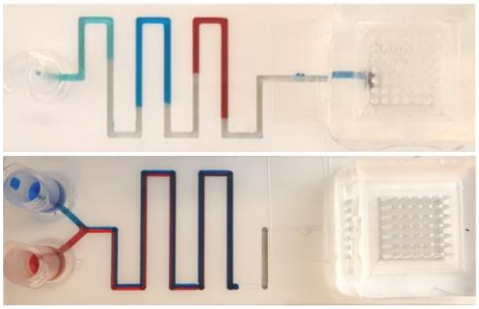

Highly versatile architecture for self-powered microfluidics adaptable to a large range of fluid volumes.